Articles in PresS. J Appl Physiol (June 1, 2017). doi:10.1152/japplphysiol.00855.2016



# Neuromuscular electrical stimulation improves skeletal muscle regeneration through satellite cell fusion with myofibers in healthy elderly subjects

Di Filippo ES[1,2], Mancinelli R[1,2,3], Marrone M[1,2], Doria C[1,2,3], Verratti V[1,3], Toniolo L[2,4], Dantas JL[3], Fulle S[1,2,3]* and Pietrangelo T[1,2,3]

[1]Department of Neuroscience Imaging and Clinical Sciences, 'G. d'Annunzio' University of Chieti–Pescara, Chieti, Italy

[2]Interuniversity Institute of Myology, Italy

[3]Laboratory of Functional Evaluation, 'G. d'Annunzio' University of Chieti–Pescara, Chieti, Italy

[4]Department of Biomedical Sciences, University of Padova, Padova, Italy

**Running head:** NMES and muscle regeneration in the elderly

***Corresponding author: Stefania Fulle**

Department of Neuroscience Imaging and Clinical Sciences

'G. d'Annunzio' University of Chieti–Pescara

Via dei Vestini, 31

66100 Chieti, Italy

Tel: +39-0871-3554555

Email: s.fulle@unich.it

## ABSTRACT

The aim was to determine whether neuromuscular electrical stimulation (NMES) affects skeletal muscle regeneration through a reduction of oxidative status in satellite cells of healthy elderly subjects. Satellite cells from the *Vastus lateralis* skeletal muscle of 12 healthy elderly subjects before and after 8 weeks of NMES were allowed to proliferate to provide myogenic populations of adult stem cells (myogenic precursor cells; MPCs). These MPCs were then investigated in terms of their proliferation, their basal cytoplasmic free $Ca^{2+}$ concentrations, and their expression of myogenic regulatory factors (*PAX3, PAX7, MYF5, MYOD, MYOG*) and microRNAs (miR-1, miR-133a/b, miR-206). The oxidative status of these MPCs was evaluated through superoxide anion production and superoxide dismutase and glutathione peroxidase activities. On dissected single skeletal myofibers, the nuclei were counted to determine the myonuclear density, the fiber phenotype, cross sectional area and tension developed. The MPCs obtained after NMES showed increased proliferation rates along with increased cytoplasmic free $Ca^{2+}$ concentrations and gene expression of *MYOD* and *MYOG* on MPCs. The muscle-specific miR-1, miR133a/b, miR-206 were up-regulated. This NMES significantly reduced superoxide anion production, along with a trend to reduction of superoxide dismutase activity. The NMES-dependent stimulation of muscle regeneration enhanced satellite cells fusion with mature skeletal fibers. NMES improved the regenerative capacity of skeletal muscle in elderly subjects. Accordingly, the skeletal muscle strength and mobility of NMES-stimulated elderly significantly improved. NMES may thus be further considered for clinical or ageing populations.

## New & Noteworthy

The NMES effect on skeletal muscle regeneration was assessed on healthy elderly for the first time. NMES improved the regenerative capacity of skeletal muscle through increased MPC proliferation and fusion with mature myofibers. The increased $[Ca^{2+}]_{cyt}$ along with *MYOD*, *MYOG* and miRNAs up-regulation could be related to reduced $O_2^{\bullet-}$ production, which, in turn, favors myogenic regeneration. Accordingly, the skeletal muscle strength of NMES-stimulated lower limbs of healthy elderly subjects improved along with their mobility.

**Keywords:** neuromuscular electrical stimulation; satellite cells; superoxide anion; oxidative status; miRNA; elderly; superoxide dismutase activity; peroxidase activity, FTSST, TUG, strength.

## Abbreviations

$[Ca^{2+}]_{cyt}$, cytoplasmic free $Ca^{2+}$ concentration; miRNA, micro ribonucleic acid; MPCs, myogenic precursor cells; NMES, neuromuscular electrical stimulation; $O_2^{\bullet-}$, superoxide anion, *MYOG*, myogenin gene; FTSST, Five Times Sit-to-Stand Test; TUG, Time to Up-and-Go test.

## INTRODUCTION

Elderly people experience skeletal muscle frailty, loss of myofibers, and dynapenia (loss of muscle strength), which in one word can be defined as sarcopenia. As a consequence, they can experience limited mobility, and, ultimately, mortality. Moreover, sarcopenia can be exacerbated by neurological deficit and/or heavy physical impairment, which, in turn, provoke immobilization. This condition often represents the point of no return in the life of the elderly, because once it is reached, these elderly people cannot perform volitional training, such as endurance or strength training, which has been shown to maintain and increase human skeletal muscle also for the elderly (25, 26, 54, 57).

In this scenario, an effective passive protocol that can be used to induce local skeletal muscle contraction, such as neuromuscular electrical stimulation (NMES), might be particularly useful to counteract the detrimental decline that occurs in sarcopenic muscle. Indeed, it is commonly accepted that NMES can offer advantages over voluntary training for people who have limited ability or are noncompliant for volitional exercise, due to its promotion of specific motor unit recruitment (20).

Effective skeletal fiber contraction involves recruitment and activation of satellite cells in the muscle (57). *In vivo*, these quiescent satellite cells of postnatal skeletal muscle fibers can be activated to the myogenic precursor cells (MPCs) that are responsible for muscle growth and repair. Although it is currently accepted that this skeletal muscle regeneration can be stimulated by exercise that involves voluntary skeletal muscle contraction, debate still remains as to whether this also

96 occurs for atypical skeletal muscle contraction, such as contraction induced by
97 NMES.

98 Administration of an electrical current in the microampere range has been
99 successfully used to rescue atrophied mouse muscle (39). Furthermore, different
100 intensities of electrical stimulation (e.g., 2-20 Hz, 0.5-20 mA; 0.3 Hz, 10 μA) can
101 stimulate the proliferation of satellite cells/MPCs and myotube activity and rescue the
102 loss of myonuclei in atrophic and damaged mouse skeletal muscle (18, 21, 52).
103 Recently, an NMES protocol was described that is particularly suited to counteract
104 disuse muscle atrophy in men (20). Considering the strict link between atrophy and
105 sarcopenia and the involvement of MPCs in both of these conditions, we investigated
106 the effects of NMES on myogenesis in elderly human subjects.

107 We have previously shown that the human regenerative potential of satellite
108 cells derived from skeletal muscle of elderly subjects can be lost through
109 spontaneous increase in the apoptotic commitment of these cells (17). Our previous
110 investigations have suggested that the increased free radical production and
111 oxidative stress that can become established in MPCs from elderly subjects can act
112 as signals for maladaptive phenomena (10, 45, 50). More specifically, accumulation
113 of the superoxide anion ($O_2^{\bullet -}$) is involved in the establishment of oxidative stress in
114 these MPCs (10). This $O_2^{\bullet -}$ is one of the most dangerous oxidant species, and it is
115 mainly produced by mitochondria that have undergone metabolic impairment (37,
116 51). Here, the key element becomes the amount of $O_2^{\bullet -}$ production and the
117 enzymatic defense that can be adopted by the cells. Indeed, low intensity training
118 mainly induces a significant $O_2^{\bullet -}$ reduction in MPCs from healthy young muscle (48).
119 However, in some subjects, this training can instead produce a slight $O_2^{\bullet -}$ increase
120 (48). In contrast, in MPCs of elderly subjects, the $O_2^{\bullet -}$ levels and the generic

cytosolic oxidation levels are at least one third more than those in MPCs of young subjects (10). This oxidative stress can provoke extensive cellular damage, apoptosis, and inflammation of skeletal fibers and the satellite cell pool (13, 14, 16). In this scenario, it is important to find stimuli that can be used to reduce the oxidative stress, in order to reduce the signals for inflammation and to promote muscle mass conservation and increased satellite cell stimulation in the elderly.

Some early evidence has demonstrated that NMES can increase intracellular defenses against reactive oxygen species in skeletal muscle of young subjects (20). Moreover, NMES has been shown to promote hypertrophy of the human *Vastus lateralis* skeletal muscle and to increase the maximal force of the quadriceps in young subjects (36). On the basis of all of this information, we asked whether NMES can influence the regeneration process and the oxidative stress of activated satellite cells (i.e., MPCs) in skeletal muscle of healthy elderly subjects. In particular, we investigated these MPCs *in-vitro*, in terms of their proliferation and differentiation into myotubes and fusion with myofibers, their basal cytoplasmic free $Ca^{2+}$ concentration ($[Ca^{2+}]_{cyt}$), and their gene expression of myogenic regulatory factors (*PAX3*, *PAX7*, *MYF5*, *MYOD*, *MYOG*) and microRNAs (miR-1, miR-133a/b, miR-206), prior to and following NMES. The oxidative status of these MPCs through $O_2^{\bullet -}$ production and the superoxide dismutase and glutathione peroxidase activities were also investigated. Moreover, the measurement of maximal voluntary contraction on elderly lower limbs permitted to relate the cellular and molecular adaptation of NMES-stimulated skeletal muscle to the effectiveness of this protocol.

## MATERIALS AND METHODS

### *Subjects*

Twelve healthy male elderly subjects (69.5 ±1.6, age) volunteered to participate in this study. They used to have an active lifestyle, but were not engaged in any specific exercise training protocols (≥6 months) before their enrolment in this study. One week before and 2 days after the NMES sessions, these subjects had their height, weight, body fat measured, and their body mass index was calculated. Their bilateral isometric maximal voluntary contraction (MVC) of the lower limbs was measured using a leg-extension device (Nessfit Srl, San Giovanni Teatino, Italy) that was equipped with loading cell to measure the strength output (Globus, Codognè, Italy). The subjects remained in a seated position on the leg-extension device with their knees at 90° and they performed a MVC for 5s using both legs. The test was performed three times and the recovery time between tests was 2 min. The highest value recorded was used as the MVC (46).

***Functional Assessment and tiny percutaneous needle biopsy***

***Five Times Sit-to-Stand Test (FTSST):*** the FTSST was applied as described in a previous study using a 43-cm high chair. After a signal from the evaluator, the volunteers stood up and sat down 5 times as quickly as possible, maintaining their arms crossed on their chest. Before the test, the evaluator provided instructions to the volunteers for a standardized execution: 1) “You need to maintain your arms crossed on your chest during the entire test”; 2) “You need to stand up and sit down 5 times as quickly as you can when I say ‘Go’”; 3) “The test begins when I say “Go” and stops when you completely touch the chair on the fifth repetition”; 4) “You need to stand up fully and touch the chair in every repetition, but you should not touch your back to chair backrest during the test” (58). Volunteers performed the FTSST three times. The first set consisted of a submaximal performance for test familiarization.

The final two sets were performed to calculate the reliability and typical error of the FTSST, the best performance being considered for the analyses.

***Timed Up and Go test (TUG):*** The TUG was applied as described in a previous study119. The volunteers were required to stand up, walk 3 m, turn, walk back, and sit down. Time to complete this task was the performance variable, evaluating mobility capacity. Two evaluators were positioned on opposite sides of the walking course (one at between 0 - 1.5m and another at between 1.5 – 3.0m) to avoid any serious consequences in the case of a fall. As in the FTSST, the volunteers performed the TUG three times, for the familiarization and reliability purposes

One day after the functional test, the tiny percutaneous needle biopsies of the *Vastus lateralis* muscles were performed. The biopsy of the VL muscle was performed at a level about one-third of the distance from the upper margin of the patella to the trochanter major. The choice of this position was motivated by the anatomical consideration that the area lacks significant neurovascular structures. For this reason the tiny percutaneous needle biopsy procedure was well tolerated. More detailed information has been extensively described in Pietrangelo et al 2011 and 2013 (43, 47).

This study was approved by the Ethics Committee of the 'G. d'Annunzio' University of Chieti–Pescara, Italy (protocol nos. 1233/06 and 1884 COET), and it was conducted according to the Helsinki Declaration. All of the subjects who participated signed their informed consent.

***Neuromuscular electrical stimulation sessions***

The NMES protocol consisted of a training program that lasted 18 min. The 12 subjects performed 40 passive isometric bilateral contractions that were stimulated

by a NMES device (Genesy 1200 Pro; Globus Srl, Codognè, Italy). This was applied for three sessions per week over an 8-week period. During the NMES session, the subjects were seated on a leg extension machine (NSFT 07036; Nessfit Srl, San Giovanni Teatino, Italy) with the knee joint fixed at 90° knee extension, to provide the isometric condition during the stimulation. Two active electrodes (contact area, 25 $cm^2$) were positioned over the motor points of the quadriceps muscles, as close as possible to the motor point of the *Vastus lateralis* and *Vastus medialis* muscles. A dispersive electrode (contact area, 50 $cm^2$) was placed 5 cm to 7 cm below the inguinal crease, to close the stimulation loop. Rectangular-wave pulsed currents (75 Hz every 400 μs) were delivered with a rise time of 1.5 s, a steady tetanic stimulation time of 4 s, and a fall time of 0.75 s (total duration of contraction, 6.25 s). A rest interval of 20 s was provided between stimulations. The intensity was monitored and recorded for each 5-min period. The intensity of the NMES was gradually increased to an individual maximally tolerable intensity, which corresponded to the pain threshold of each subject. The subjects were motivated to adjust their intensity during the training session to maintain the maximum tolerable intensity throughout the session, reaching at the end of the training period an intensity of 40 ±16 mA.

***Satellite cell population and myogenicity***

A part of the tiny percutaneous muscle biopsies (about 10 mg) was treated to obtain the muscle cells (43). The progeny of *in-vitro* satellite cells, MPCs, were initially expanded in growth medium, and differentiated into myotubes as previously described (15, 45, 48). These MPCs from the *Vastus lateralis* of the 12 healthy elderly subjects were obtained before the NMES sessions were started, and after

220 they were completed, with these samples defined as pre-NMES and post-NMES,
221 respectively.

222 Briefly, the percentages of myogenicity were obtained by counting the MPCs
223 that were positive for an antibody against desmin (15), with respect to all of the cells
224 present in the field of view. We counted 6341 and 6369 cells on pre- and post-NMES
225 samples, respectively. At a confluence of 70% to 80%, the cells were split and the
226 population doubling level (PDL) was calculated. This is given by the ratio between
227 the number of cells that were detached (Nd) with respect to the number of cells that
228 were initially seeded (Ns; i.e., Nd/Ns), and log Nd/Ns was calculated and divided by
229 ln 2. The MPCs controls derived from TPNB samples of subjects without NMES were
230 analyzed as previously described.

231 The differentiation of these MPCs into myotubes was measured in terms of
232 the multinucleated cells that were positive to the primary antibody against myosin
233 heavy chain after 7 days of differentiation. This is reported as the Fusion Index, as a
234 percentage defined by counting the numbers of nuclei present in the myotubes, with
235 respect to the total number of nuclei in the observed field (i.e., nuclei in myotubes/
236 total nuclei ×100%). Myotubes were defined as those that were positive to the
237 primary antibody against myosin heavy chain and that had at least two nuclei (48).
238 We counted 2717 and 2731 cells on pre- and post-NMES samples, respectively.
239 Moreover, in the samples that were differentiated for 7 days, the numbers of
240 mononucleated desmin$^{+}$ cells were counted, which represents the number of
241 myogenic cells that were not able to fuse into multinucleated myotubes. We counted
242 2150 and 2139 cells on pre- and post-NMES samples, respectively.
243

244 ***Myonuclear density of single myofibers***

Another part of the tiny percutaneous muscle biopsies (about 5 mg) from four of these subjects was manually dissected to obtain single skeletal myofibers (47). The myonuclei along these single myofibers were counted, to determine the nuclear domain. Briefly, to localize the nuclei, single myofibers were stained with DAPI (25 µg/mL; Sigma) for 10 min. To precisely measure the volume, the fibers have been stained with a monoclonal mouse antibody anti-$\alpha$-actinin (clone EA-53 Sigma). The myonuclear density was determined as the number of nuclei in a constant myofiber volume ($10^6$ µm$^3$). A confocal microscope (Vico; Nikon) was used to acquire the fluorescent images (32, 40).

***Mechanical features and phenotype of single fibers***

Muscle biopsy fragments for single fiber were stored at -20˚C and analyzed within 2 weeks of sampling. The biopsies were stored in skinning solution with 50% (v/v) glycerol until day of the experiment. This solution contains high-potassium and high-EGTA concentration that depolarizes membranes, removes calcium, and induces a rigor to ensuring optimal conditions for fiber preservation. Before the analysis, the skinning-glycerol mixture was replaced with ice-cold skinning solution containing ATP, to induce fiber relaxation. From each biopsy single fibers were manually dissected using a stereo-microscope (x10-60 magnification). Following dissection, fibers were bathed for 10 min in skinning solution containing 1% (v/v) Triton X-100 to completely have the membranes in solution. Fiber segments of 1-2 mm in length were cut, and light aluminum clips were applied at both ends. Then they were transferred to the experimental apparatus, and cross-sectional area (CSA) and tension development during maximal calcium-activated isometric contractions at 12˚C were measured according to a previously described procedure (56, 41). At the

end of the experiment, each fiber was collected and put in Laemmli solution for electrophoretic analysis (see below). All solutions employed for single fiber experiments were prepared as described previously (7).

***Electrophoretic separation and quantification of myosin heavy chain isoforms***

The fibers were characterized for their myosin heavy chain **(**MyHC) isoform. Muscle biopsy fragments were solubilized in an appropriate volume of Laemmli solution (Tris 62.5 mM, Glycerol 10% [v/v], SDS 2.3% [w/v], ß-mercaptoethanol 5% [v/v], with E-64 0.1% [w/v] and leupeptin 0.1% [w/v] as anti-proteolytic factors; pH 6.8) and stored at -80 °C until the analysis. Appropriate amounts (~10 µg of total protein/lane) of the protein suspension were diluted in loading buffer (Laemmli solution with 0,01% bromophenol blue) and boiled for 5 min at 80˚C before loading onto polyacrylamide gels. Separation of MyHC isoforms was carried out on 8% (w/v) gels (18 cm x 16 cm x 1 mm) at 70 V for 1.5 h and at 230 V for a further time according to the guidelines of Talmadge and Roy (1993). The gels were stained with Coomassie-blue dye. After staining, three separate bands were detected in the 200-kDa region, corresponding to MyHC-1, -2A, and -2X, in order of migration from fastest to slowest. For each biopsy sample fragment, at least two independent electrophoretic runs were performed. Gel patterns were digitized with an HP Scanjet G4050 at a resolution of 1,200 dpi. The myosin isoforms distribution was achieved by densitometric analyses of the bands after staining with Coomassie-blue. Each band was characterized by a value of the Brightness-Area Product (BAP), after black/white inversion employing LI-COR®Image Studio Lite (ver 5.0). From each line, BAP values for the bands identified as MyHC isoforms were summed and the BAP value for each isoform was expressed as a percentage of the total and the mean values of myosin isoforms

295 distribution for all subjects were obtained. The reproducibility of the procedure was
296 confirmed by calculating isoform ratios of selected samples from gels loaded with
297 different amounts of such samples.
298
299 ***Intracellular calcium concentrations***
300 The MPCs were loaded with Fura2-AM (final concentration, 5 μM) for 30 min,
301 washed by gentle solution removal and incubated for a further 30 min at 37 °C prior
302 to the $[Ca^{2+}]_{cyt}$ measurements, to allow the intracellular Fura2-AM de-esterification
303 (27). The experiments were performed and images were acquired using the
304 procedures and set-up described by Pietrangelo et al. (44). Thapsigargin (1 μM;
305 Sigma-Aldrich T9033), a known releaser of internal $Ca^{2+}$ stores, was added in the
306 MPCs to induce the emptying of the intracellular $Ca^{2+}$ stores. The thapsigargin-
307 dependent $[Ca^{2+}]_{cyt}$ transients was recorded for at least 2 min, and analysis of the
308 area under the 2-min transients was performed using the specific 'area under the
309 curve' function of GraphPad Prism Software, version 5 (GraphPad Software, La Jolla,
310 USA).
311
312 ***Reactive oxygen species***
313 The superoxide anion ($O_2\bullet^-$) levels were determined using the conventional assay
314 based on the dye nitroblue tetrazolium chloride (Cat. No. N6639; Sigma-Aldrich),
315 which is reduced to formazan by $O_2\bullet^-$, determined at 550 nm using a fluorometer
316 (SPECTRAmax Gemini XS; Molecular Devices Toronto, Canada (10, 48).
317 The cellular oxidant levels were determined using the dye 2,7-
318 dichlorofluorescein diacetate (DCF, Cat.No. D6883; Sigma). The fluorescence was
319 determined at 530 nm (excitation, 490 nm) using a fluorometer (SPECTRAmax

Gemini XS; Molecular Devices Toronto, Canada), with the data analyzed using the SOFTmax Pro software (48).

***Antioxidant enzyme activity***

The antioxidant enzyme activities of superoxide dismutase and glutathione peroxidase (53, 55) were analyzed for the cytosolic fractions of undifferentiated MPCs. The superoxide dismutase activity, where 2 $O_2^{\bullet -}$ (+ 2 $H^+$) is oxidized to form $O_2$ and $H_2O_2$, was determined as previously described (48). The glutathione peroxidase enzymatic activity was determined according to Shakirzyanova et al. (53), and reported as specific activities.

***Western blotting***

Western blotting (WB) analysis was performed on 40 $\mu$g lysates from pre- and post-NMES MPCs, using SOD1 (71G8) mouse mAb (#4266, Cell Signalling Technology, Danvers, MA, USA) at 1:1000, SOD2 (D9V9C) rabbit mAb (#13194, Cell Signalling Technology) at 1:1000, β-Actin (8H10D10) mouse mAb (#3700, Cell Signalling Technology) at 1:1000, as primary antibody. Secondary HRP-conjugated antibodies (Cell Signalling Technology) at 1:5000. Bands were detected and pictured at Bio-Rad GelDoc by LiteAblot PLUS enhanced chemiluminiscent substrate (EuroClone); densitometry analyses were performed with ImageJ software (10).

***Quantitative real-time PCR for myogenic transcriptional factors and miRNAs***

The RNA was extracted from the PMCs using Purelink RNA mini kits (Invitrogen, Life Technologies), as described by Di Filippo et al. (10). Briefly, 500 ng extracted RNA was reverse transcribed using Superscript III First-Strand Synthesis SuperMix kits

(Invitrogen, Life Technologies). Quantitative real-time PCR was performed on 1:5 diluted cDNA, using Platinum Sybr Green SuperMix-UDG (Invitrogen, Life Technologies). The myogenic regulatory factors investigated were: *PAX3, PAX7, MYF5, MYOD, and MYOG*. GAPDH was used as the housekeeping gene, and the data are shown as ΔCt.

PureLink miRNA isolation kits were used for the miRNA extractions (Cat. No. K1570-01; Invitrogen, Life Technologies, Molecular Devices, Sunnyvale, USA), according to Di Filippo et al. (10). The relative quantification of the miRNA targets was carried out using the ΔCt formula. The specific miRNA sequence probes used have the following catalog numbers: hsa-miR-16-5p, #000391; hsa-miR-1, #002222; hsa-miR-206, #000510; hsa-miR-133b, #002247; hsa-miR-133a, #002246. miR-16 was used as the housekeeping gene, and the data are shown as ΔCt. Three independent experiments were performed, each carried out in triplicate.

***Statistical analysis***

The statistical analysis was carried out using the GraphPad Prism Software, version 5 (GraphPad Software, La Jolla, USA). The data are reported as means ± standard error (SE) or standard deviation (SD). Unpaired and paired t-tests were used to reveal statistical differences between cellular populations and single myofiber analysis, respectively, at pre- and post-NMES.

Mixed analysis of variance (mixed ANOVA) was used to analyze differences between groups and over time (control vs NMES-stimulated elderly) in addition to Bonferroni post hoc comparisons.

Significance was indicated as *p ≤0.05, **p ≤0.005, and ***p ≤0.0001.

## RESULTS

### *Maximal voluntary contraction of elderly subjects*

The anthropometric characteristics of the 12 healthy elderly subjects who participated in the NMES sessions did not vary significantly (Table 1). However, compared to the pre-NMES maximal voluntary contractions, the post-NMES values showed a significant increase as well as the FTSST and TUG (Table 1).

Table 1 to be inserted about here

### *Myogenic characteristics and analysis of MPC differentiation*

The myogenic characteristics of the MPCs are reported in Table 2. Here, from pre-NMES to post-NMES, there were no significant differences in the MPC myogenicity (i.e., number of desmin$^+$ cells), Fusion Index, and desmin$^+$ nonfused MPCs at 7 days of differentiation, as for control samples (data not shown).

Table 2 to be inserted about here

### *Proliferation rate* in vitro

The PDLs of the pre-NMES and post-NMES MPCs were calculated at each passage, when the cells reached about 80% confluence. As can be seen in Figure 1, the pre-NMES MPCs reached 10 PDL in 50 days to 120 days (panel a), while the post-NMES MPCs of the same subjects reached the same PDL in 30 days to 35 days

(panel b), demonstrating an increased rate of MPC proliferation post-NMES, similar for all subjects. The MPCs controls, without NMES stimulation, reached 10 PDL in 35-40 days, showing a similar proliferation trend of pre-NMES MPCs (data not shown).

Figure 1 to be inserted about here

***Myonuclear density on single mature myofibers***

The single mature myofibers showed significant increases from pre-NMES to post-NMES for the myonuclei fused to the myofibers ($p \leq 0.05$; Figure 2).

Figure 2 to be inserted about here

***MyHC fiber phenotype***

The fiber type composition of the *Vastus Lateralis* muscle was determined by analyzing the proportion of slow (MyHC-1) and fast (MyHC-2A and -2X) myosin heavy chain isoforms in pre- and post-NMES biopsy samples. The average percentage of fibers that express the specific MyHC isoform are shown in Figure 3. In our sample, slow MyHC-1 fibers were significantly increased in post-NMES compared to pre-NMES ($p \leq 0.05$). The percentage of fast MyHC-2A fibers did not significantly vary whereas that of MyHC-2X ones showed a decrease not statistically significant.

Figure 3 to be inserted about here

420

421 ***Muscle fiber cross-sectional area and specific tension***

422 The results on single muscle fibers (n=80) are displayed in the Figure 4. The CSA
423 was significantly incremented at post-NMES *vs* pre-NMES (5,810±267 $\mu m^2$ *vs*
424 4,983±288 $\mu m^2$, $p \leq 0.05$). The average force ($F_o$) significantly increased of about
425 20%, from 1.06±0.06 mN to 1.25±0.05 in post-NMES ($p \leq 0.05$).
426 The value of specific tension (Po), the isometric strength per unit of fiber area
427 ($F_o$/CSA), was 126.0±6.7 mN $mm^{-2}$ and 137.8±7.7 mN $mm^{-2}$ in pre- and post-NMES,
428 respectively. Although $P_o$ tended to increase, this increment was not statistically
429 significant.

430

431 Figure 4 to be inserted about here

432

433 ***Cytoplasmic free $Ca^{2+}$ concentrations of undifferentiated MPCs***

434 The basal $[Ca^{2+}]_{cyt}$ were significantly increased in the undifferentiated MPCs from
435 pre-NMES to post-NMES ($p \leq 0.05$; Figure 5a). The analysis of the time courses of
436 the $Ca^{2+}$ released from the intracellular stores by thapsigargin (Figure 5b)
437 demonstrated that in these undifferentiated MPCs, from pre-NMES to post-NMES,
438 there was less $Ca^{2+}$ released. The analysis of the area under the curve for these
439 thapsigargin-dependent $[Ca^{2+}]_{cyt}$ changes from pre-NMES to post-NMES showed a
440 significant reduction ($p \leq 0.001$; Figure 5c).

441

442 Figure 5 to be inserted about here

443

444 ***Myogenic regulatory factor gene expression profiles***

For the undifferentiated MPCs, from pre-NMES to post-NMES, the myogenic transcription factors *PAX3, PAX7, MYF5* did not change their expression levels, while *MYOD* and *MYOG* were significantly up-regulated ($p \leq 0.05$ and $p \leq 0.0001$, respectively; Figure 6).

Figure 6 to be inserted about here

***Superoxide anion production and basal levels of oxidant species***

The undifferentiated MPCs from pre-NMES to post-NMES showed significant $O_2^{\bullet -}$ decrease (by about 40%) (Figure 7a).

The DCF fluorescence did not vary significantly from pre-NMES to post-NMES (data not shown).

***Antioxidant enzyme activity***

The activity of the cytosolic fractions from pre-NMES to post-NMES for the antioxidant enzyme superoxide dismutase showed a decrease trend (31.8 ±1.4 *vs.* 29.7 ±1 U superoxide dismutase $ng^{-1}$; Figure 7b). Instead, the glutathione peroxidase enzymatic activity remained the same from pre-NMES to post-NMES (0.25 ±0.06 *vs*. 0.27 ±0.05, data not shown).

Figure 7 to be inserted about here

***SOD1 and SOD2 protein expression***.

A representative SOD1 and SOD2 bands obtained by MPCs at pre- and post-NMES was shown in Figure 8a. The amount of both SOD cytosolic type 1 and mitochondrial type 2 were reported in Figure 8b and c, by Western blotting analysis.

Figure 8 to be inserted about here

**Epigenetic miRNA profile**

The analysis of the miRNA expression from pre-NMES to post-NMES showed significant up-regulation of miR-1, miR-133a, miR-133b and miR-206 ($p \leq 0.0001$; Figure 9).

Figure 9 to be inserted about here

**DISCUSSION**

The lowered regenerative potential of satellite cells that occurs during human ageing is known to be linked to the accumulation of oxidant species like $O_2^{\bullet -}$, together with inadequate scavenger activity. These effects provoke cellular damage and impair the ability of satellite cells to efficiently divide to the MPCs that can differentiate to sustain muscle mass and function (5, 10, 12, 15, 30, 45). The hypothesis for the present study was that NMES positively stimulates skeletal muscle regeneration of healthy elderly subjects through a reduction in the MPC oxidation levels.

The data here for the MPC populations obtained after the NMES (i.e., post-NMES) suggest that this procedure can promote increased proliferation rate along with increased fusion of these adult stem cells with the existing myofibers.

We investigated some of the potential molecular aspects as key elements of this regeneration process, in terms of $[Ca^{2+}]_{cyt}$ homeostasis, muscle regulating transcription factors and miRNA expression, and oxidative species management.

In these undifferentiated MPCs, these data showed a post-NMES reduction in the $[Ca^{2+}]_{cyt}$ of the (thapsigargin-releasable) intracellular $Ca^{2+}$ stores in favor of an increase in the basal $[Ca^{2+}]_{cyt}$. This is in line with the increased ability of these post-NMES MPCs to fuse with existing myofibers (6, 27, 29). The release of the free $Ca^{2+}$ from intracellular stores occurs during the early steps of myoblast differentiation (3), when a proliferative boost is required (33, 42). On this basis, our data confirm the increased proliferation rate in the post-NMES MPCs. The NMES-dependent $[Ca^{2+}]_{cyt}$ increase might influence the fusion process via two key $Ca^{2+}$-dependent enzymes, the transcription factor nuclear factor of activated T cells (NFAT) and the protein kinase CamKII, which stimulate myogenin (2). Indeed an increase in $[Ca^{2+}]_{cyt}$ is required for activation of myogenic transcription factors, such as myogenin (1). Accordingly, myogenin gene expression was significantly up-regulated here. It is also worth mentioning that this gene was not linked to myotube formation, because the Fusion Index was similar here between the pre-NMES and post-NMES MPCs, although we believe that it is instrumental for MPC fusion with existing myofibers. Indeed, the post-NMES MPCs showed increased proliferation rate along with no MYF5, PAX3 and *PAX7* variation but *MYOD* overexpression, with respect to pre-NMES MPCs. It has been extensively demonstrated that this specific transcription factor regulation occur when MPCs were committed to fusion escaping the self-renewal (8).

Considering the importance of oxidative stress in human satellite cells, and its role in impairment of regenerative processes in the elderly, we investigated the redox

balance of these pre-NMES and post-NMES MPCs. Surprisingly, the post-NMES MPCs showed significant reduction (about 40%) in $O_2^{\bullet -}$ production even in the presence of increased number of MyHC-1 fibers, the slow ones, those that rely mostly on mitochondrial oxidative metabolism.

Superoxide dismutase and glutathione peroxidase are the most important antioxidant enzymes for detoxification of $O_2^{\bullet -}$ and its derivative $H_2O_2$, respectively, but these did not show different activities between the pre-NMES to post-NMES MPCs. Moreover, the reduced trend of superoxide dismutase activity is in agreement with both the decreased $O_2^{\bullet -}$ production and the mitochondrial SOD2 protein reduction we found on post-NMES MPCs. Superoxide dismutase reduces $O_2^{\bullet -}$ to $H_2O_2$, which is then a substrate for glutathione peroxidase. In the present study, the glutathione peroxidase activity did not change. It might be that $H_2O_2$ that was also produced through oxygen reduction by other metabolic sources did not decrease with the $O_2^{\bullet -}$, and as a consequence, the glutathione peroxidase activity of the post-NMES MPCs remained similar to that of the pre-NMES MPCs. In accordance, the data on general cellular peroxidation performed using DCF fluorescence, revealed that the cellular peroxidation end products measured directly on cells did not vary between pre- and post-NMES. It may be that the period of 8 weeks of stimulation was not sufficient to reduce the MPC general oxidative state in elderly, as expected considering the $O_2^{\bullet -}$ reduction. Under another point of view, it is also interesting that the general oxidation did not increase even in the presence of increased percentage of oxidative MyHC-1 fiber, that confirms data on NMES-dependent atypical fiber adaptation already present in literature (20). Moreover, it could be that NMES protocol has to be performed with other strategies, such as active training, to reduce MPC general oxidation (4). Interestingly, the increased proportion of MyHC-1 fibers

542 at post-NMES along with reduced $O_2^{\bullet -}$ production and no interference with the
543 oxidative status, let think that NMES could be an healthy treatment for elderly.

544 The idea that miRNAs may regulate and be regulated by oxidative stress
545 following active and/or passive exercise in skeletal muscle still awaits experimental
546 validation. However, in other cellular model such as neuron, endothelial,
547 cardiomyocytes it has been established a specific miRNA regulation by oxidant level
548 (28, 35, 59). Yildirim and coworkers (60) demonstrated a relationship between
549 increase of oxidative stress and down-regulation of miR-1, miR-133a and miR-133b
550 in rat cardiomyocytes.

551 Recently, we demonstrated human regulation of miRNAs by $O_2^{\bullet -}$ production
552 linked to low-intensity exercise. Indeed, we observed that human MPCs that
553 decreased $O_2^{\bullet -}$ production showed up-regulation of miR-1, miR-133b and miR-206,
554 while those that increased $O_2^{\bullet -}$ showed down-regulation of these myo-miRNAs (34,
555 48).

556 Accordingly, the decreased $O_2^{\bullet -}$ production up-regulated these myo-miRNAs,
557 along with miR-133a, which promoted (or supported) the myogenesis process, and
558 confirmed the positive role of the NMES protocol.

559 Nakasa and colleagues (38) demonstrated that local injection of miR-1, miR-
560 133 and miR-206 mixture in rat skeletal muscle increased muscle regeneration via
561 increased myogenic regulator factors as myogenin. Furthermore, up-regulation of
562 miR-1, miR-133a/b and miR-206 might be linked to reduction of muscle inflammation
563 (19), which would also be consistent with a reduction in the $O_2^{\bullet -}$ levels as a positive
564 effect of the NMES protocol. Moreover, it has been demonstrated that miR-133 and
565 miR-1 expression is linked to the regulation of apoptotic pathways (10). Although we
566 did not obtain information about this specific pathway here, we believe that the up-

regulation of both miR-1 and miR-133a/b could be in line with apoptosis repression, in favor of cell proliferation (9, 24, 48).

One of the most important effects of stimulation of the skeletal muscle regeneration process, which in the present case relates to MPC fusion with myofibers, is the increased cross sectional area and isometric strength of myofibers, and as a direct consequence, the increase in muscle strength. The isometric maximal voluntary strength of lower limbs measured on post-NMES significantly increased with respect to pre-NMES, accordingly with the present literature (11, 23). Interestingly, we found other NMES positive effects on elderly mobility, as revealed by FTSST and TUG functional tests. These effects reveal an important physiological outcome of this NMES-dependent activation of skeletal muscle regeneration and suggest that NMES may thus be further considered for counteract sarcopenia. Indeed, even if one limitation of this method could be the discomfort that is associated with the intensity of the electrically-induced muscle contractions (31, 23), in our experience, the NMES has been well tolerated by elderly. Moreover, NMES could be considered as an important adjuvant in clinical approach for those individuals who are unable to exercise because of orthopedic problems or other complications also considering the positive effect reported in literature on energy expenditure and human metabolism enhancement (22, 49).

## CONCLUSIONS

Neuromuscular electrical stimulation is an interesting protocol for the stimulation of human skeletal muscle, even if this is achieved passively and in a localized manner. Although NMES is extensively used in sport and human muscle rehabilitation, there

592 is little evidence of the physiological effects and few data on regeneration of human
593 sarcopenic muscle. We have demonstrated in the present study that NMES
594 stimulates specific physiological signals for MPC regeneration, which can result in
595 increased fusion of satellite cells with existing mature myofibers of the elderly through
596 increases in $[Ca^{2+}]_{cyt}$. This process appears to be driven by overexpression of
597 myogenin that is sustained by up-regulation of myo-miRNAs, which can occur due to
598 reduced $O_2^{\bullet -}$ production in the MPCs stimulated by this NMES protocol. In
599 conclusion, this NMES can help muscle regeneration and increase the maximal
600 isometric strength of the lower limbs in healthy elderly subjects along with their
601 mobility.
602

603 **ACKNOWLEDGMENTS**

604 The authors would like to thank all of the subjects who volunteered to participate in
605 this study for their collaboration. The authors thank Dr Christopher Berrie for English
606 editing. This study was funded by 'G. d'Annunzio' University grants to TP, RM and
607 SF, and the PRIN national grants 2007AWZTHH_003 to SF and 2012N8YJC3_003
608 to TP.
609

610 **CONFLICTS OF INTEREST**

611 The authors declare that they have no conflicts of interest.
612

613 **REFERENCES**

614

615 1. **Antigny F, Koenig S, Bernheim L, Frieden M.** During post-natal human
616 myogenesis, normal myotube size requires TRPC1- and TRPC4-mediated $Ca^{2+}$
617 entry. *J Cell Sci* 126: 2525-2533, 2013. doi: 10.1242/jcs.122911.
618 2. **Antigny F, Konig S, Bernheim L, Frieden M.** Inositol 1,4,5 trisphosphate
619 receptor 1 is a key player of human myoblast differentiation. *Cell Calcium* 56:
620 513-521, 2014. doi: 10.1016/j.ceca.2014.10.014.
621 3. **Arnaudeau S, Holzer N, König S, Bader CR, and Bernheim L.** Calcium sources
622 used by post-natal human myoblasts during initial differentiation. *J Cell Physiol*
623 208: 435-445, 2006.
624 4. **Baar K.** Using molecular biology to maximize concurrent training. *Sports Med* 44:
625 S117-125, 2014 doi: 10.1007/s40279-014-0252-0.
626 5. **Beccafico S, Puglielli C, Pietrangelo T, Bellomo R, Fanò G, and Fulle S.** Age-
627 dependent effects on functional aspects in human satellite cells. *Ann N Y Acad*
628 *Sci* 1100: 345-352, 2007.
629 6. **Bijlenga P, Liu JH, Espinos E, Haenggeli CA, Fischer-Lougheed J, Bader CR,**
630 **and Bernheim L.** T-type alpha 1H $Ca^{2+}$ channels are involved in $Ca^{2+}$ signaling
631 during terminal differentiation (fusion) of human myoblasts. *Proc Natl Acad Sci*
632 *USA* 97: 7627-7632, 2000. doi: 10.1073/pnas.97.13.7627.
633 7. **Bottinelli R, Canepari M, Pellegrino MA, Reggiani C.** Force-velocity properties
634 of human skeletal muscle fibers: myosin heavy chain isoform and temperature
635 dependence. *J Physiol* 495: 573-586, 1996.
636 8. **Ceafalan LC, Popescu BO, and Hinescu ME**. Cellular Players in Skeletal Muscle
637 Regeneration. *BioMed Research International* Volume 2014, Article ID 957014,
638 2014. doi.org/10.1155/2014/957014

9. **Crippa S, Cassano M, and Sampaolesi M**. Role of miRNAs in Muscle Stem Cell Biology: Proliferation Differentiation and Death. *Current Pharmaceutical Design* 18: 1718-1729, 2012.

10. **Di Filippo ES, Mancinelli R, Pietrangelo T, La Rovere RM, Quattrocelli M, Sampaolesi M, and Fulle S.** Myomir dysregulation and reactive oxygen species in aged human satellite cells. *Biochem Biophys Res Commun* 473: 462-470, 2016. doi: 10.1016/j.bbrc.2016.03.030

11. **Filipovic A, Kleinöder H, Dörmann U, Mester J**. Electromyostimulation--a systematic review of the effects of different electromyostimulation methods on selected strength parameters in trained and elite athletes. *J Strength Cond Res* 26: 2600-2614, 2012.

12. **Fisher-Wellman K, and Bloomer J**. Acute exercise and oxidative stress: a 30 year history. *Dynamic Medicine* 8: 1, 2009. doi: 10.1186/1476-5918-8-1

13. **Franceschi C, and Campisi J.** Chronic inflammation (inflammaging) and its potential contribution to age-associated diseases. *J Gerontol A Biol Sci Med Sci* 69 Suppl 1: S4-9, 2014. doi: 10.1093/gerona/glu057

14. **Fulle S, Mecocci P, Fanó G, Vecchiet I, Vecchini A, Racciotti D**, **Cherubini A, Pizzigallo E, Vecchiet L, Senin U, and Beal MF**. Specific oxidative alterations in vastus lateralis muscle of patients with the diagnosis of chronic fatigue syndrome. *Free Radic Biol Med* 29: 1252-1259, 2000.

15. **Fulle S, Di Donna S, Puglielli C, Pietrangelo T, Beccafico S, Bellomo R**, **Protasi F, and Fanò G.** Age-dependent imbalance of the antioxidative system in human satellite cells. *Exp Gerontol* 40: 189-197, 2005.

16. **Fulle S, Pietrangelo T, Mancinelli R, Saggini R, and Fanò G.** Specific correlations between muscle oxidative stress and chronic fatigue syndrome: a working hypothesis. *J Muscle Res Cell Motil* 28: 355-362, 2007.

17. **Fulle S, Sancilio S, Mancinelli R, Gatta V, and Di Pietro R.** Dual role of the caspase enzymes in satellite cells from aged and young subjects. *Cell Death Dis* 4: e955, 2013. doi: 10.1038/cddis.2013.472

18. **Fujiya H, Ogura Y, Ohno Y, Goto A, Nakamura A, Ohashi K, Uematsu D, Aoki H, Musha H, and Goto K**. Microcurrent Electrical Neuromuscular Stimulation Facilitates Regeneration of Injured Skeletal Muscle in Mice. *Journal of Sports Science and Medicine* 14: 297-303, 2015.

19. **Georgantas RW, Streicher K, Greenberg SA, Greenlees LM, Zhu W, Brohawn PZ, Higgs BW, Czapiga M, Morehouse CA, Amato A, Richman L, Jallal B, Yao Y, and Ranade K.** Inhibition of myogenic microRNAs 1, 133, and 206 by inflammatory cytokines links inflammation and muscle degeneration in adult inflammatory myopathies. *Arthritis Rheumatol* 66: 1022-1033, 2014. doi: 10.1002/art.38292.

20. **Gondin J, Brocca L, Bellinzona E, D'Antona G, Maffiuletti NA, Miotti D, Pellegrino MA, Bottinelli R.** Neuromuscular electrical stimulation training induces atypical adaptations of the human skeletal muscle phenotype: a functional and proteomic analysis. *J Appl Physiol* 110: 433–450, 2011. doi: 10.1152/japplphysiol.00914.2010.

21. **Guo BS, Cheung KK, Yeung SS, Zhang BT, and Yeung EW.** Electrical stimulation influences satellite cell proliferation and apoptosis in unloading-induced muscle atrophy in mice. *PLoS ONE* 7, e30348, 2012.

687 22. **Hamada T, Hayashi T, Kimura T, Nakao K, Moritani T**. Electrical stimulation of
688 human lower extremities enhances energy consumption, carbohydrate oxidation,
689 and whole body glucose uptake. *J Appl Physiol (1985)*. 96(3):911-916, 2004.
690 23. **Herzig D, Maffiuletti NA, Eser P**. The application of neuromuscular electrical
691 stimulation training in various non-neurological patient populations: a narrative
692 review. *Physical Medicine and Rehabilitation* 7:1167-1178, 2015.
693 24. **Huang ZP, Espinoza-Lewis R, and Wang DZ.** Determination of miRNA targets
694 in skeletal muscle cells. *Methods Mol Biol* 798: 475–490, 2012.
695 25. **Kadi F, Johansson F, Johansson R, Sjöström M, and Henriksson J.** Effects
696 of one bout of endurance exercise on the expression of myogenin in human
697 quadriceps muscle. *Histochem Cell Biol* 121: 329-334, 2004.
698 26. **Kvorning T, Kadi F, Schjerling P, Andersen M, Brixen K, Suetta C, and**
699 **Madsen K.** The activity of satellite cells and myonuclei following 8 weeks of
700 strength training in young men with suppressed testosterone levels. *Acta Physiol*
701 *(Oxf)* 213: 676-687, 2015. doi: 10.1111/apha.12404.
702 27. **La Rovere RML, Quattrocelli M, Pietrangelo T, Di Filippo ES, Maccatrozzo L,**
703 **Cassano M, Mascarello F, Barthélémy I, Blot S, Sampaolesi M, and Fulle S.**
704 Myogenic potential of canine craniofacial satellite cells. *Frontiers Aging Neurosci*
705 6: 90, 2014. doi: 10.3389/fnagi.2014.00090
706 28. **Li R, Yan G, Li Q, Sun H, Hu Y, Sun J, and Xu B.** MicroRNA-145 protects
707 cardiomyocytes against hydrogen peroxide ($H_2O_2$)- induced apoptosis through
708 targeting the mitochondria apoptotic pathway. *PLoS One* 7(9): e44907, 2012. doi:
709 10.1371/journal.pone.0044907.

29. **Liu JH, König S, Michel M, Arnaudeau S, Fischer-Lougheed J, Bader CR, and Bernheim L.** Acceleration of human myoblast fusion by depolarization: graded $Ca^{2+}$ signals involved. *Development* 130: 3437-3446, 2003.

30. **Lorenzon P, Bandi E, de Guarrini F, Pietrangelo T, Schäfer R, Zweyer M, Wernig A, and Ruzzier F.** Ageing affects the differentiation potential of human myoblasts. *Exp Gerontol* 39: 1545-1554, 2004.

31. **Maffiuletti NA**. Physiological and methodological considerations for the use of neuromuscular electrical stimulation.*Eur J Appl Physiol*. 110(2):223-234, 2010. doi: 10.1007/s00421-010-1502-y.

32. **Mancinelli R, Pietrangelo T, La Rovere R, Toniolo L, Fanò G, Reggiani C, and Fulle S.** Cellular and molecular responses of human skeletal muscle exposed to hypoxic environment. *J Biol Regul Homeost Agents* 25: 635-645, 2011.

33. **Mancinelli R, Pietrangelo T, Burnstock G, Fanò G, and Fulle S.** Transcriptional profile of GTP-mediated differentiation of C2C12 skeletal muscle cells. *Purinergic Signal* 8: 207–221, 2012. doi: 10.1007/s11302-011-9266-3

34. **Mancinelli R, DiFilippo ES, Verratti V, Fulle S, Toniolo L, Reggiani C, and Pietrangelo T.** The regenerative potential of female skeletal muscle upon hypobaric hypoxic exposure. *Front Physiol* 7: 303, 2016. doi: 10.3389/fphys.2016.00303

35. **Marin T, Gongol B, Chen Z, Woo B, Subramaniam S, Chien S, and Shyy JY.** Mechanosensitive microRNAs-role in endothelial responses to shear stress and redox state. *Free Radic Biol Med* 64: 61-68, 2013. doi: 10.1016/j.freeradbiomed.2013.05.034

734 36. **Minetto MA, Botter A, Bottinelli O, Miotti D, Bottinelli R, and D'Antona G.**
735 Variability in muscle adaptation to electrical stimulation. *Int J Sports Med* 34: 544-
736 553, 2013. doi: 10.1055/s-0032-1321799.
737 37. **Muller FL, Liu Y, and Van Remmen H.** Complex III releases superoxide to both
738 sides of inner mitochondrial membrane. *J Biol Chem* 279: 49064-49073, 2004.
739 doi:10.1074/jbc.M407715200
740 38. **Nakasa T, Ishikawa M, Shi M, Shibuya H, Adachi N, and Ochi M.** Acceleration
741 of muscle regeneration by local injection of muscle-specific microRNAs in rat
742 skeletal muscle injury model. *J Cell Mol Med* 14: 2495-2505, 2010.
743 39. **Ohno Y, Fujiya H, Goto A, Nakamura A, Nishiura Y, Sugiura T, Ohira Y,**
744 **Yoshioka T and Goto K.** Microcurrent electrical nerve stimulation facilitates
745 regrowth of mouse soleus muscle. *International Journal of Medical Sciences* 10:
746 1286-1294, 2013.
747 40**. Paoli A, Pacelli QF, Cancellara P, Toniolo L, Moro T, Canato M, Miotti D**
748 **and Reggiani C**. Myosin isoforms and contractile properties of single fibers of
749 human Latissimus Dorsi muscle**.** *Biomed Res Int*. 2013:249398, 2013 doi:
750 10.1155/2013/249398.
751 41. **Pellegrino MA, Canepari M, D'Antona G, Reggiani C, Bottinelli R**.
752 Orthologous myosin isoforms and scaling of shortening velocity with body size in
753 mouse, rat, rabbit and human muscles. *J Physiol* 546:677-689, 2003.
754 42. **Pietrangelo T, Fioretti B, Mancinelli R, Catacuzzeno L, Franciolini F, Fanò G,**
755 **and Fulle S.** Extracellular guanosine-5'-triphosphate modulates myogenesis via
756 intermediate Ca($^{2+}$)-activated $K^+$ currents in C2C12 mouse cells. *J Physiol* 572(Pt
757 3): 721-733, 2006.

758 43. **Pietrangelo T, D'Amelio L, Doria C, Mancinelli R, Fulle S, and Fanò G.** Tiny
759 percutaneous needle biopsy: an efficient method for studying cellular and
760 molecular aspects of skeletal muscle in humans. *Int J Mol Med* 27: 361-367,
761 2011.
762 44. **Pietrangelo T, Mariggiò MA, Lorenzon P, Fulle S, Protasi F, Rathbone M.,**
763 **Werstiuk E, and Fanò G.** Characterization of specific GTP binding sites in
764 C2C12 mouse skeletal muscle cells. *J Muscle Res Cell Motil* 23: 107-118, 2002.
765 45. **Pietrangelo T, Puglielli C, Mancinelli R, Beccafico S, Fanò G, and Fulle S.**
766 Molecular basis of the Myogenic profile of aged human skeletal muscle satellite
767 cells during differentiation. *Exp Geront* 44: 523-531, 2009.
768 46. **Pietrangelo T, Mancinelli R, Doria C, Di Tano G, Loffredo B, Fanò-Illic G and**
769 **Fulle S.** Endurance and resistance training modifies the transcriptional profile of
770 the vastus lateralis skeletal muscle in healthy elderly subjects. *Sport Sci Health*
771 7: 19–27, 2012. doi: 10.1007/s11332-012-0107-8
772 47. **Pietrangelo T, Perni S, Di Tano G, Fanò-Illic G. and Franzini-Armstrong C.** A
773 method for the ultrastructural preservation of tiny percutaneous needle biopsy
774 material from skeletal muscle. *Int. J Mol Med* 32: 965-970, 2013.
775 doi:10.3892/ijmm.2013.1454
776 48. **Pietrangelo T, Di Filippo ES, Mancinelli R, Doria C, Rotini A, Fanò-Illic G.**
777 **and Fulle S.** Low Intensity Exercise Training Improves Skeletal Muscle
778 Regeneration Potential. *Front Physiol* 6:399,
779 2015.doi:10.3389/fphys.2015.00399.
780 49. **Porcelli S, Marzorati M, Pugliese L, Adamo S, Gondin J, Bottinelli R, Grassi**
781 **B**. Lack of functional effects of neuromuscular electrical stimulation on skeletal

muscle oxidative metabolism in healthy humans. *J Appl Physiol (1985)*. 113(7):1101-1109, 2012. doi: 10.1152/japplphysiol.01627.2011.

50. **Powers SK, Duarte J, Kavazis AN, and Talbert EE.** Reactive oxygen species are signaling molecules for skeletal muscle adaptation. *Exp Physiol* 95: 1-9, 2010.

51. **Quinlan CL, Perevoshchikova IV, Hey-Mogensen M, Orr AL, and Brand MD.** Sites of reactive oxygen species generation by mitochondria oxidizing different substrates. *Redox Biol* 1: 304-312, 2013.

52. **Sciancalepore M, Coslovich T, Lorenzon P, Ziraldo G, Taccola G**. Extracellular stimulation with human “noisy” electromyographic patterns facilitates myotube activity. *J Muscle Res Cell Motil*, 36: 349-357, 2015. DOI 10.1007/s10974-015-9424-2

53. **Shakirzyanova A, Valeeva G, Giniatullin A, Naumenko N, Fulle S, Akulov A, Atalay M, Nikolsky E, and Giniatullin R.** Age-dependent action of reactive oxygen species on transmitter release in mammalian neuromuscular junctions. *Neurobiol Aging* 38: 73-81, 2016. doi: 10.1016/j.neurobiolaging.2015.10.02

54. **Snijders T, Verdijk LB, Beelen M, McKay BR, Parise G, Kadi F, and van Loon LJ.** A single bout of exercise activates skeletal muscle satellite cells during subsequent overnight recovery. *Exp Physiol* 97: 762-773, 2012. doi: 10.1113/expphysiol.2011.063313

55. **Sullivan-Gunn MJ, and Lewandowski PA.** Elevated hydrogen peroxide and decreased catalase and glutathione peroxidase protection are associated with aging sarcopenia. *BMC Geriatr* 13: 104, 2013. doi: 10.1186/1471-2318-13-104.

56. **Toniolo L, Maccatrozzo L, and Patruno M**. Fiber types in canine muscles: myosin isoform expression and functional characterization. *Am J Physiol* 292:C1915-C1926, 2007.

57. **Verdijk LB.** Satellite cells activation as a critical step in skeletal muscle plasticity. *Exp Physiol* 99, 1449–1450, 2014. doi: 10.1113/expphysiol.2014. 081273.

58. **Whitney SL, Wrisley DM, Marchetti GF, Gee MA, Redfern MS, Furman JM**. Clinical measurement of sit-to-stand performance in people with balance disorders: validity of data for the Five-Times-Sit-to-Stand Test. *Phys Ther.* 85(10):1034-45, 2005

59. **Xu S, Zhang R, Niu J, Cui D, Xie B, Zhang B, Lu K, Yu W, Wang X, Zhang Q.** Oxidative Stress Mediated-Alterations of the MicroRNA Expression Profile in Mouse Hippocampal Neurons. *Int J Mol Sci* 13: 16945–16960, 2012. doi: 10.3390/ijms131216945

60. **Yildirim SS, Akman D, Catalucci D, and Turan B.** Relationship between downregulation of miRNAs and increase of oxidative stress in the development of diabetic cardiac dysfunction: junctin as a target protein of miR-1. *Cell Biochem Biophys* 67: 1397-1408, 2013. doi: 10.1007/s12013-013-9672-y.

**Table 1:** Anthropometric characteristics, isometric maximal voluntary contraction (MVC) of lower limb and functional performance measured on healthy elderly subjects before (Pre-) and after (Post-) the neuromuscular electrical stimulation (NMES) protocol.

| | NMES | | CONTROL | |
|---|---|---|---|---|
| **Characteristic** | **Pre** | **Post** | **Pre** | **Post** |
| Weight (kg) | 74.2±6.9 | 74.5±7.0 | 76.8±4.2 | 77.5±4.0 |
| Height (m) | 1.65±0.06 | 1.65±0.06 | 1.66±0.03 | 1.66±0.03 |
| BMI (kg/m$^2$) | 27.3±2.7 | 27.4±2.8 | 27.9±2.2 | 28.2±2.1 |
| Body fat (%) | 26.7±5.1 | 25.6±5.2 | 24.8±3.5 | 24.7±3.6 |
| MVC (N) | 546±126 | 605±118* | 499±137 | 488±125 |
| FSST (s) | 7.96±0.71 | 6.50±0.30** | 7.55±0.98 | 7.43±1.14 |
| TUG (s) | 6.02±1.15 | 4.71±0.51*** | 5.33±0.52 | 5.45±0.49 |

* Significant difference for interaction time*group for NMES (n=14) *vs* Control (n=8) group (F(12642.574)= 5.014; P= 0.037; np$^2$= 0.200; 1-β= 0.568)

** Significant difference between Pre and Post for NMES group (n= 5; F(4.056, 1.962)= 24.811; P= 0.001; np$^2$= 0.674; 1-β= 0.995) and interaction time*group for NMES (n=5) vs Control (n=9) group (F(2.866, 1.962)= 17.529; P= 0.001; np$^2$= 0.594; 1-β= 0.969)

*** Significant difference between Pre and Post for NMES group (n= 4; F(1.972, 1.289)= 16.823; P= 0.002; np$^2$= 0.605; 1-β= 0.961) and interaction time*group for NMES (n=4) vs Control (n=9) group (F(2.818, 1.289)= 24.044; P= 0.001; np$^2$= 0.686; 1-β= 0.993).

BMI, body mass index; BF, body fat; MVC, muscle voluntary contraction; N, Newton; FSST, Five Times Sit-to-Stand Test; TUG, Timed Up and Go test.

847 **Table 2.** Myogenicity and differentiation features of the MPCs isolated from the
848 *Vastus Lateralis* of the healthy elderly subjects before (Pre-) and after (Post-) the
849 NMES sessions.
850

| Condition | Myogenicity | Differentiation | |
|---|---|---|---|
| | (%desmin$^+$) | Fusion Index (%) | %Desmin$^+$ unfused |
| Pre-NMES | 64.9 ±4.5 | 46.7 ±6.9 | 57.0 ±9.6 |
| Post-NMES | 71.1 ±5.4 | 50.7 ±6.2 | 50.7 ±8.6 |

851
852
853
854 **Figure legends**
855
856 **Figure 1**. **Population doubling level of MPCs.**
857 Population doubling levels of MPCs (undifferentiated cells) obtained from the skeletal
858 muscle of six representative of the healthy elderly subjects, with respect to the days
859 of *in-vitro* cultivation of these cells, as pre-NMES (a) and post-NMES (b).
860
861 **Figure 2. Myonuclei fused with single mature myofibers.**
862 The graph shows the numbers of myonuclei for the single dissected myofibers from
863 the muscle needle biopsy of elderly subjects were counted (per $10^6$ $\mu m^3$ myofiber
864 volume). The myofibers analyzed were 27 and 33 for pre- and post-NMES samples,
865 respectively. The images show an example of human fibers stained for determination
866 of myonuclear density: the nuclei are revealed with DAPI; an antibody against alpha-
867 actinin allows to determine the volume. Top, image of pre-NMES myofiber; bottom,
868 image of post-NMES myofiber. Scale bar, 20 μm.

**Figure 3. MyHC isoform distribution in biopsy samples collected before and after NMES.** The MyHC isoform distribution was determined by electrophoretic separation and densitometric analysis of proteins of biopsy samples from the *Vastus Lateralis* muscle. The dark columns represent the percentages of the MyHC isoform distribution on post-NMES, and the white columns represent pre-NMES percentages. *p≤0.05.

**Figure 4. Phenotype and isometric tension of single fiber**

Single-fiber analysis, cross sectional area (A), force (B) and specific isometric tension (C). The white and dark columns represent pre-NMES and post-NMES samples, respectively. Panel A shows the cross-sectional area (CSA) of single muscle fibers obtained by the *Vastus Lateralis*. Panel B shows the force developed by single fiber. Panel C reported measurements of specific isometric tension (force/CSA) developed in maximal calcium activated contraction by the same fibers. *p ≤0.05

**Figure 5. Free intracellular $Ca^{2+}$ concentrations of MPCs.**

(a) Free cytoplasmic $Ca^{2+}$ concentrations of the undifferentiated MPCs as pre-NMES to post-NMES, as the basal $[Ca^{2+}]_{cyt}$ (*, p <0.05) and (b) the time-course of the thapsigargin-dependent $Ca^{2+}$ release. (c) Area under the curve measures for the $[Ca^{2+}]_{cyt}$ of the undifferentiated MPCs, as pre-NMES to post-NMES, for estimation of the thapsigargin-sensitive $Ca^{2+}$ stores released over the first 2 min of thapsigargin stimulation (***, p < 0.0001).

**Figure 6. Gene expression of early transcriptional and myogenic regulatory factors**.

Pre-NMES to post-NMES mRNA expression levels (as ΔCt) for *Pax3*, *Pax7*, *Myf5*, *MyoD*, and *myogenin* gene expression. Data are means ± SE from three independent experiments, each performed in triplicate. (*, p <0.05 and ***, p <0.0001)

**Figure 7. Superoxide anion production and superoxide enzymatic dismutation.**

Quantitative analyses from pre-NMES to post-NMES in MPCs for $O_2^{\bullet-}$ (a) and the activity of the enzyme superoxide dismutase, SOD (b). The SOD units ($U_{SOD}$) were calculated considering that 1 SOD unit is defined as the quantity that inhibits the rate of cytochrome c reduction by 50% per ng of protein (b). ***, p <0.0001

**Figure 8. SOD1 and SOD2 protein expression.**

Western blotting analysis of superoxide enzymes cytosolic type 1, and mitochondrial type 2. The panel a shows representative bands of SOD1 and SOD2 enzymes obtained by MPCs from *Vastus Lateralis* muscles biopsies before (pre-) and after (post-) NMES. Panel b and c show the SOD2 and SOD1 protein quantification.

*, p <0.05, n=4

**Figure 9**. **miRNA expression**.

Pre-NMES to post-NMES relative expression (as ΔCt) of miR-133a, miR-133b, miRNA-1, and miR-206 (as indicated) in MPCs. Data are means ± SE from three independent experiments, each performed in triplicate. ***, p <0.0001

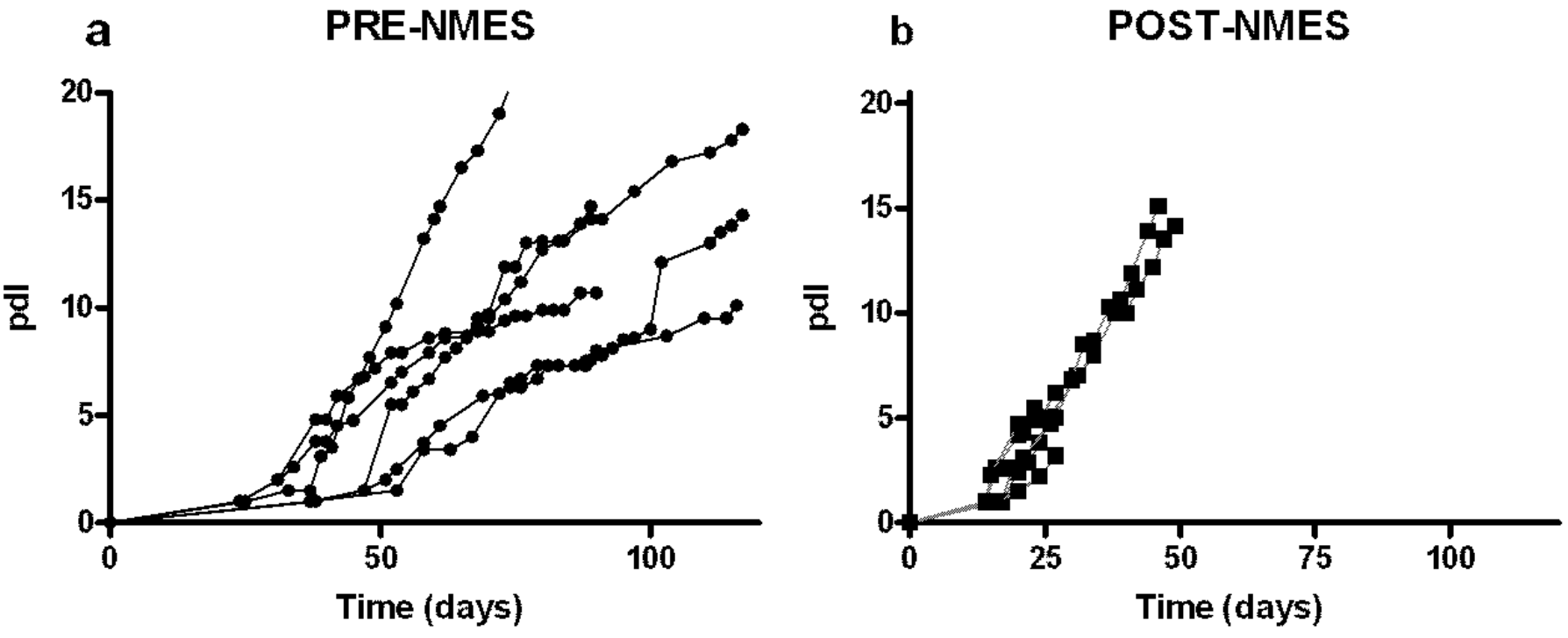
a
PRE-NMES
pdl
20
15
10
5
0
0
50
100
Time (days)
b
POST-NMES
pdl
20
15
10
5
0
0
25
50
75
100
Time (days)

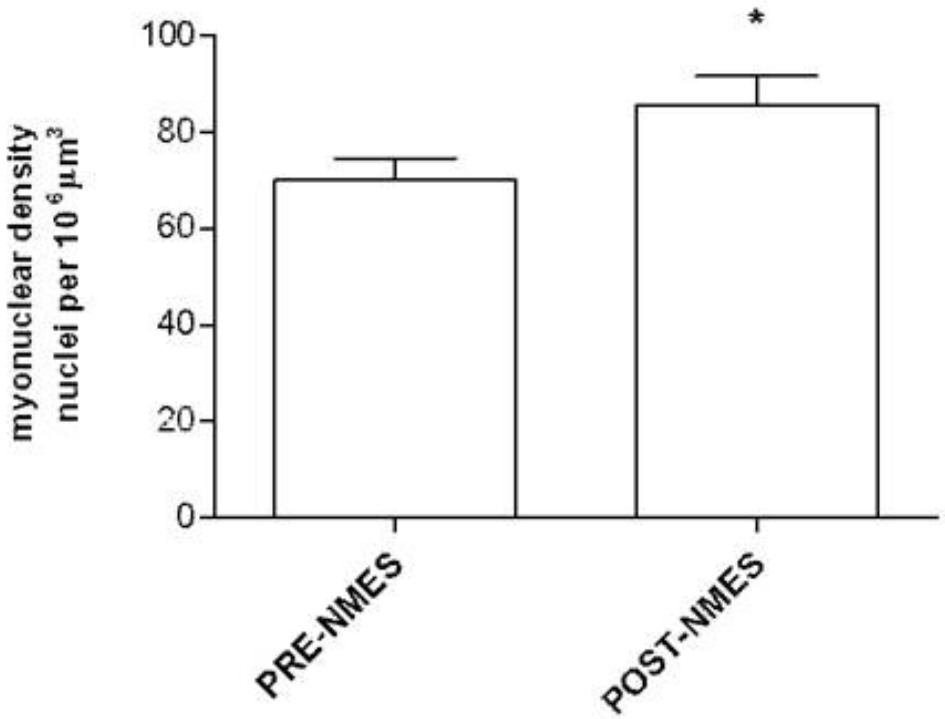


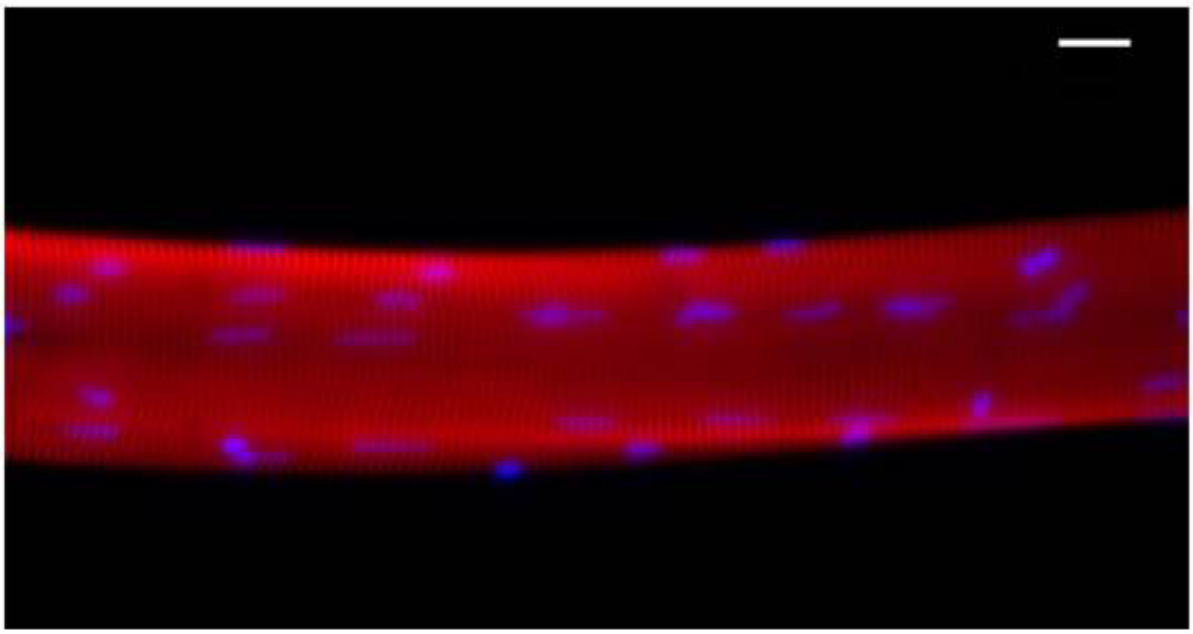

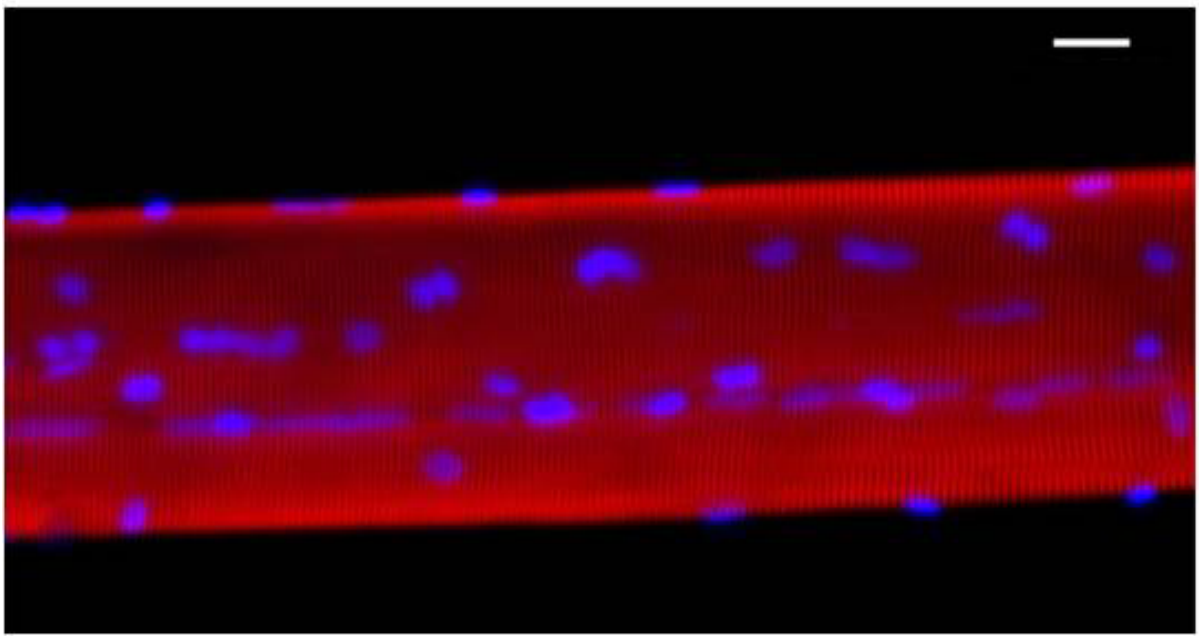

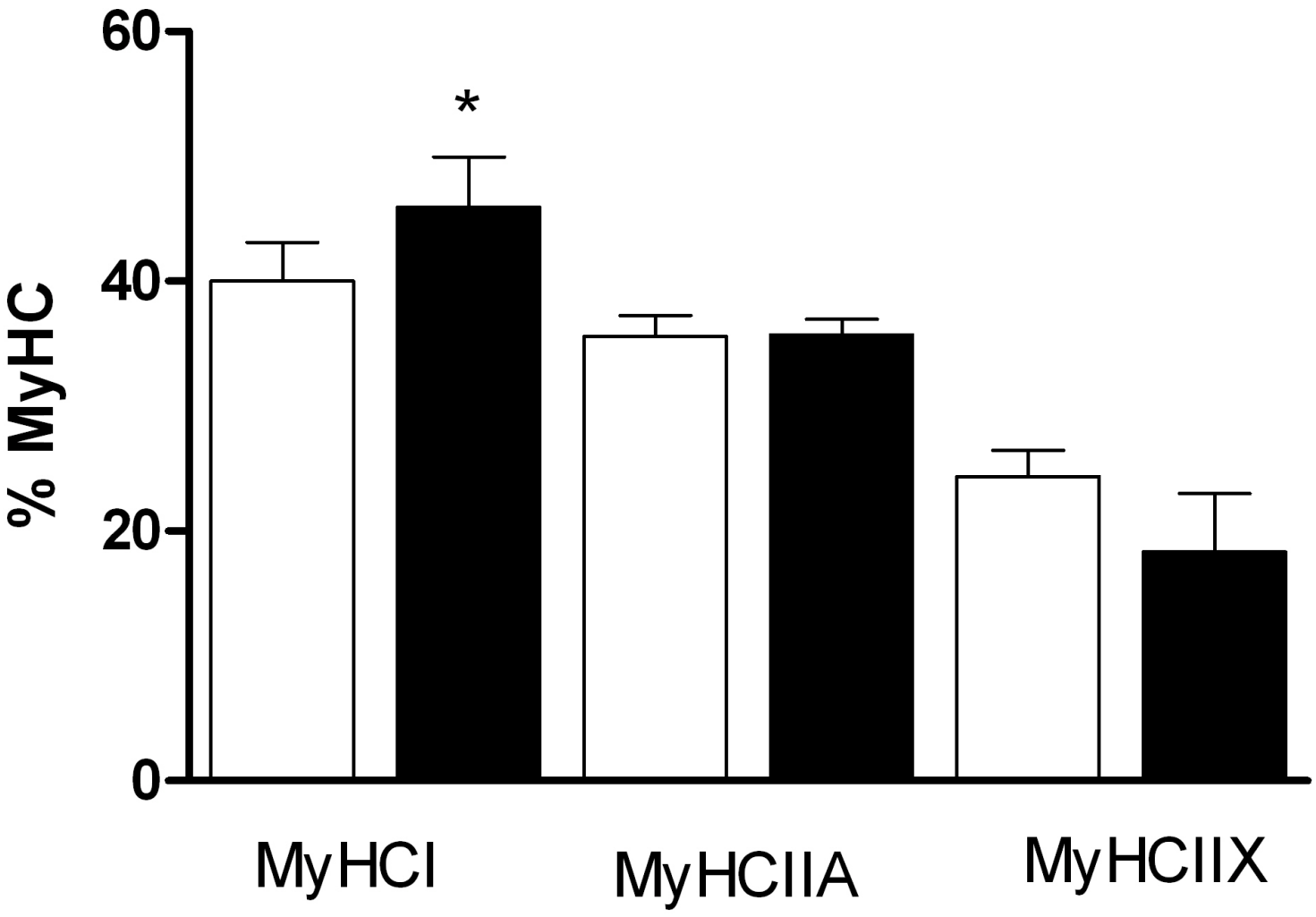

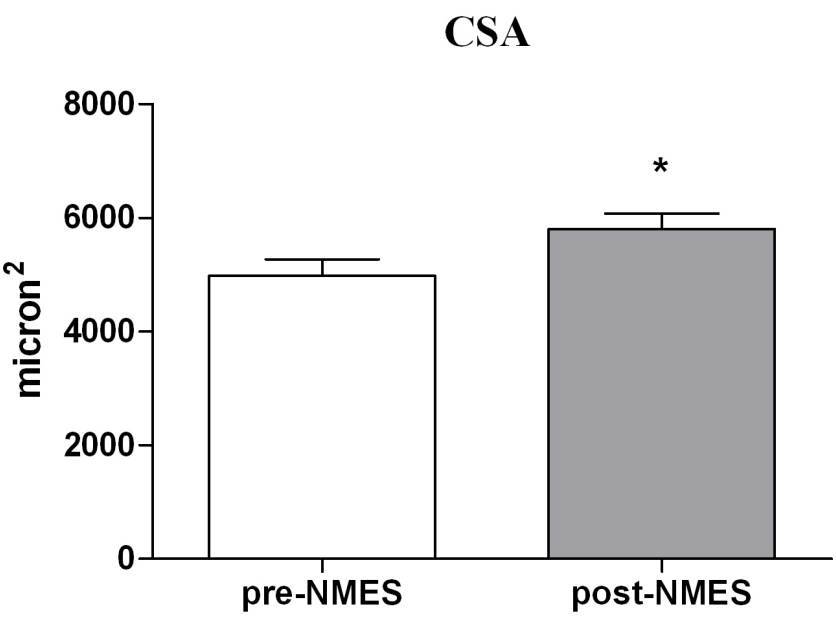


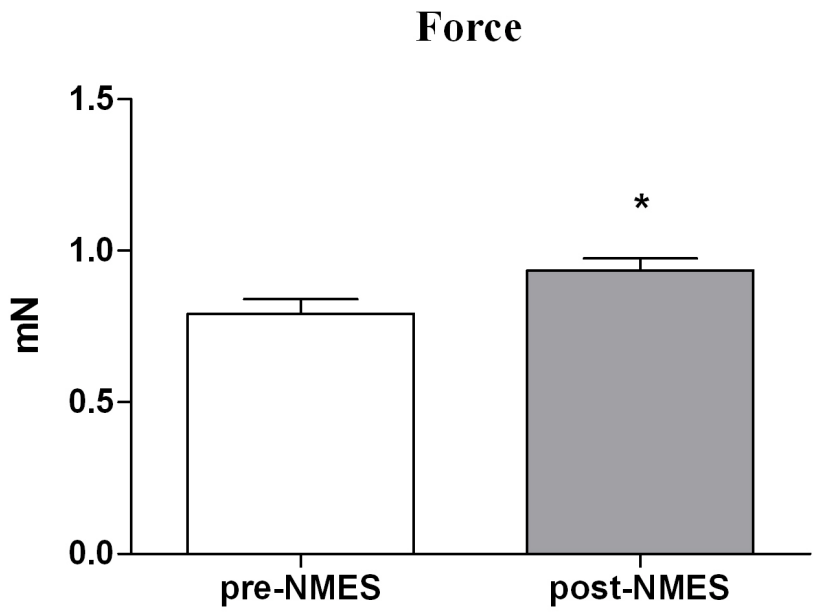


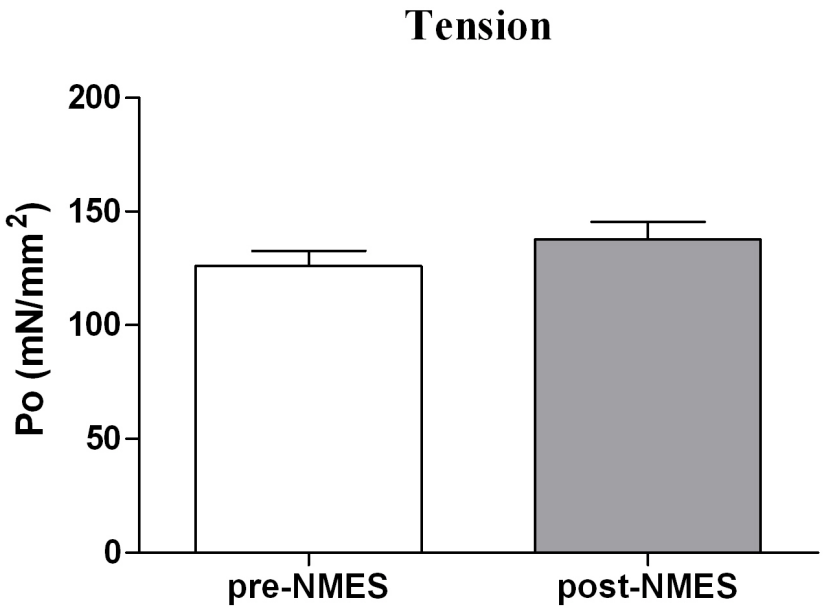

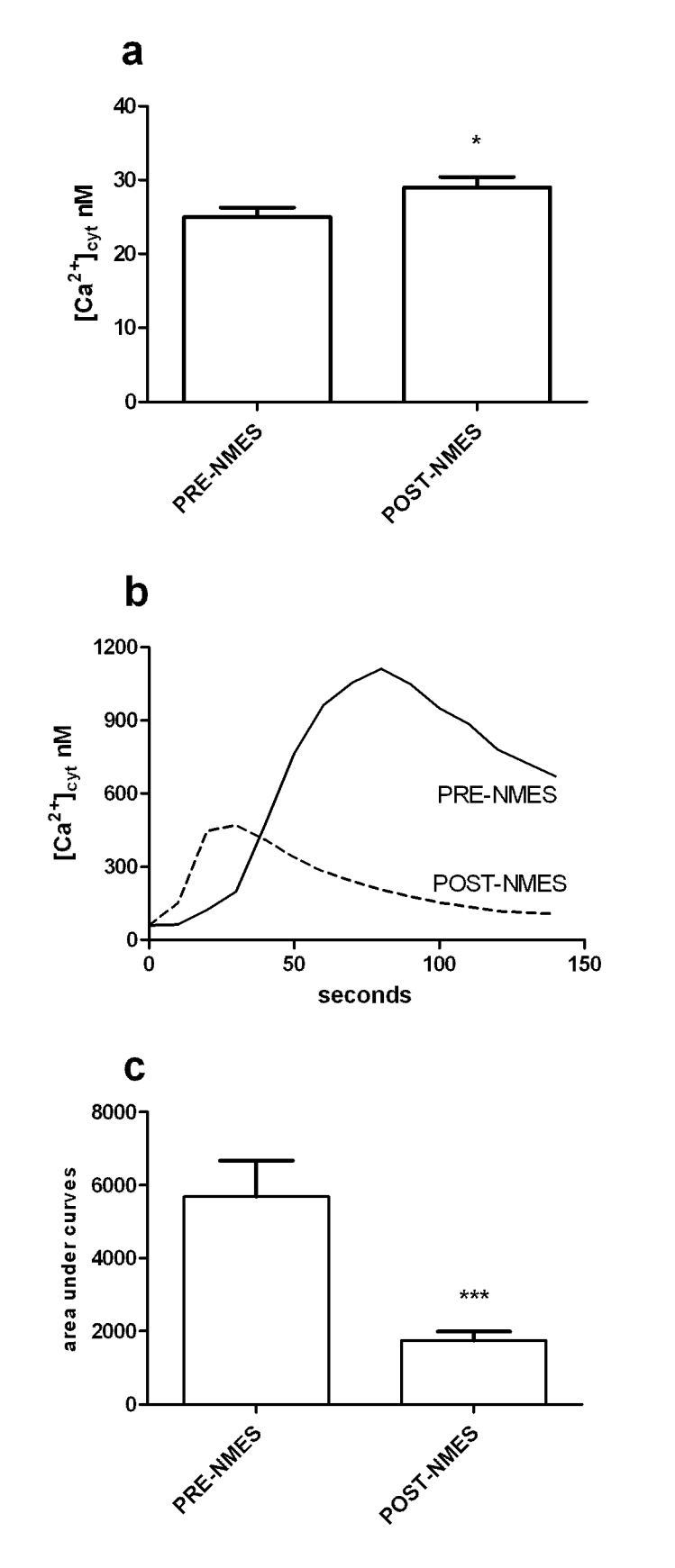
a
40
30
20
10
0
[Ca2+]cyt nM
*
PRE-NMES
POST-NMES
b
1200
900
600
300
0
[Ca2+]cyt nM
PRE-NMES
POST-NMES
0
50
100
150
seconds
c
8000
6000
4000
2000
0
area under curves
***
PRE-NMES
POST-NMES

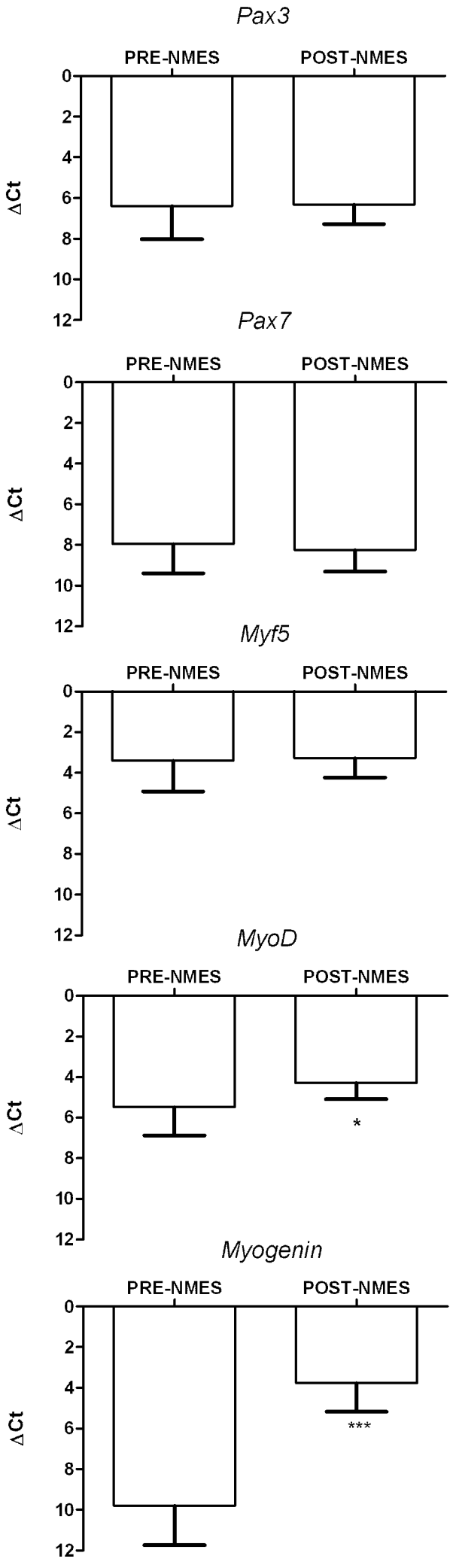
Pax3
PRE-NMES
POST-NMES
ΔCt
0
2
4
6
8
10
12
Pax7
PRE-NMES
POST-NMES
ΔCt
0
2
4
6
8
10
12
Myf5
PRE-NMES
POST-NMES
ΔCt
0
2
4
6
8
10
12
MyoD
PRE-NMES
POST-NMES
*
ΔCt
0
2
4
6
8
10
12
Myogenin
PRE-NMES
POST-NMES
***
ΔCt
0
2
4
6
8
10
12

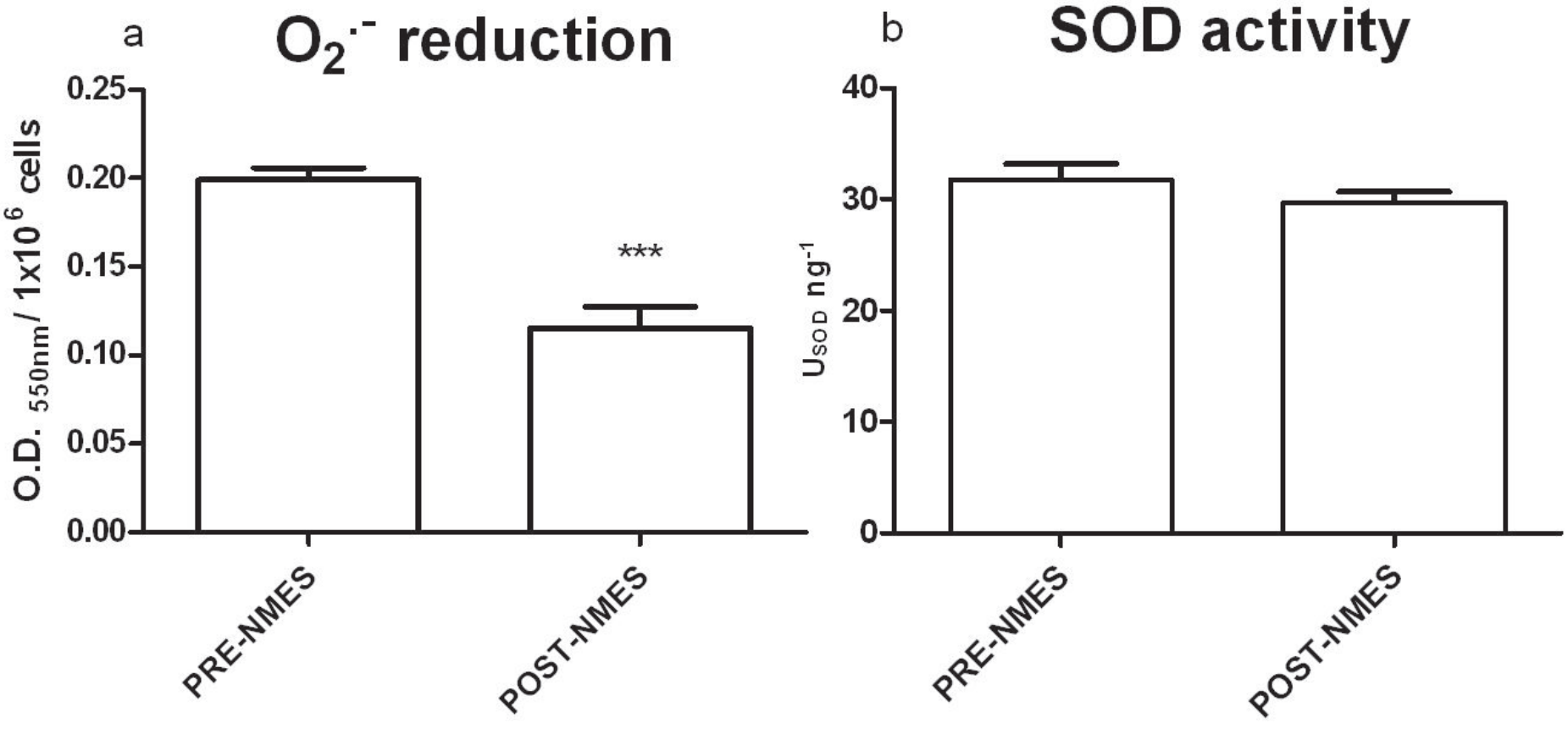
a
$O_2^{\cdot -}$ reduction
O.D. 550nm/ 1x10$^6$ cells
0.25
0.20
0.15
0.10
0.05
0.00
***
PRE-NMES
POST-NMES
b
SOD activity
$U_{SOD}$ ng$^{-1}$
40
30
20
10
0
PRE-NMES
POST-NMES

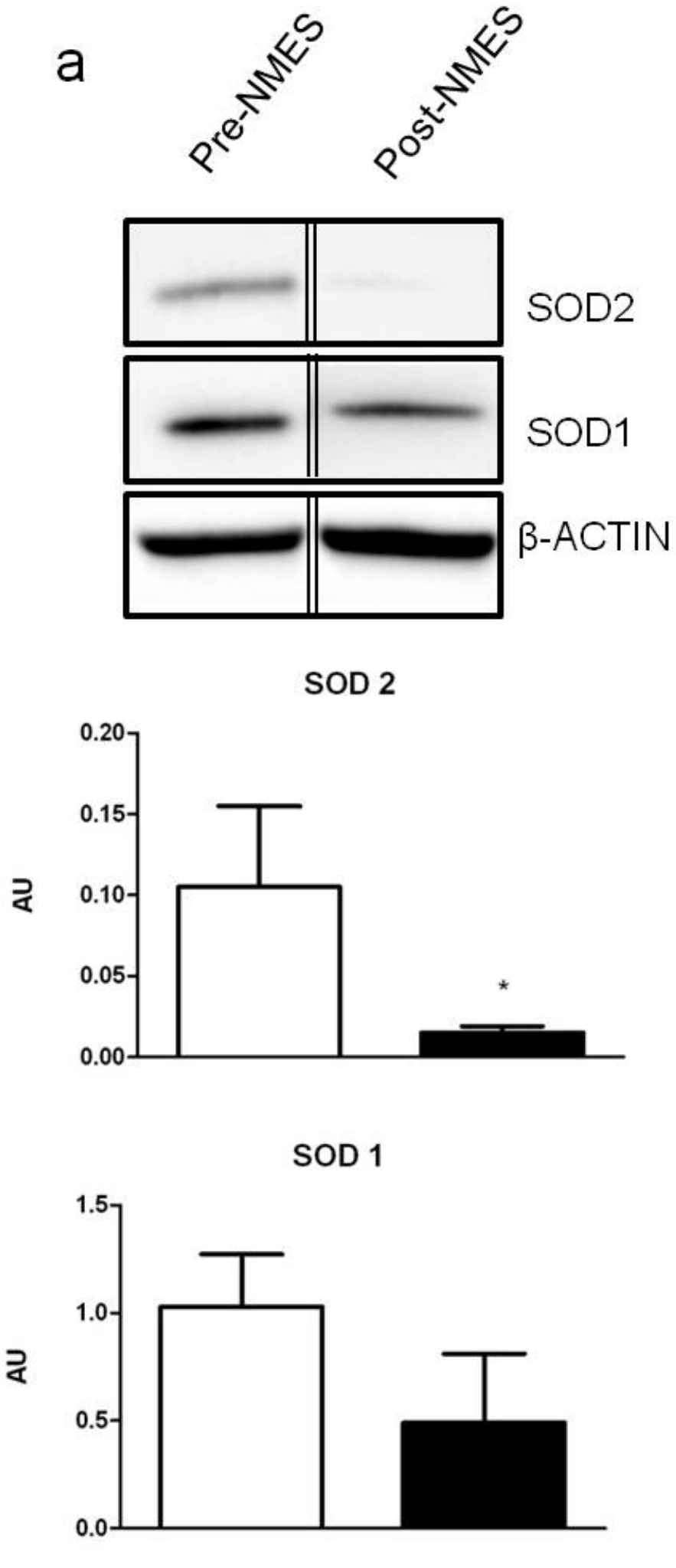

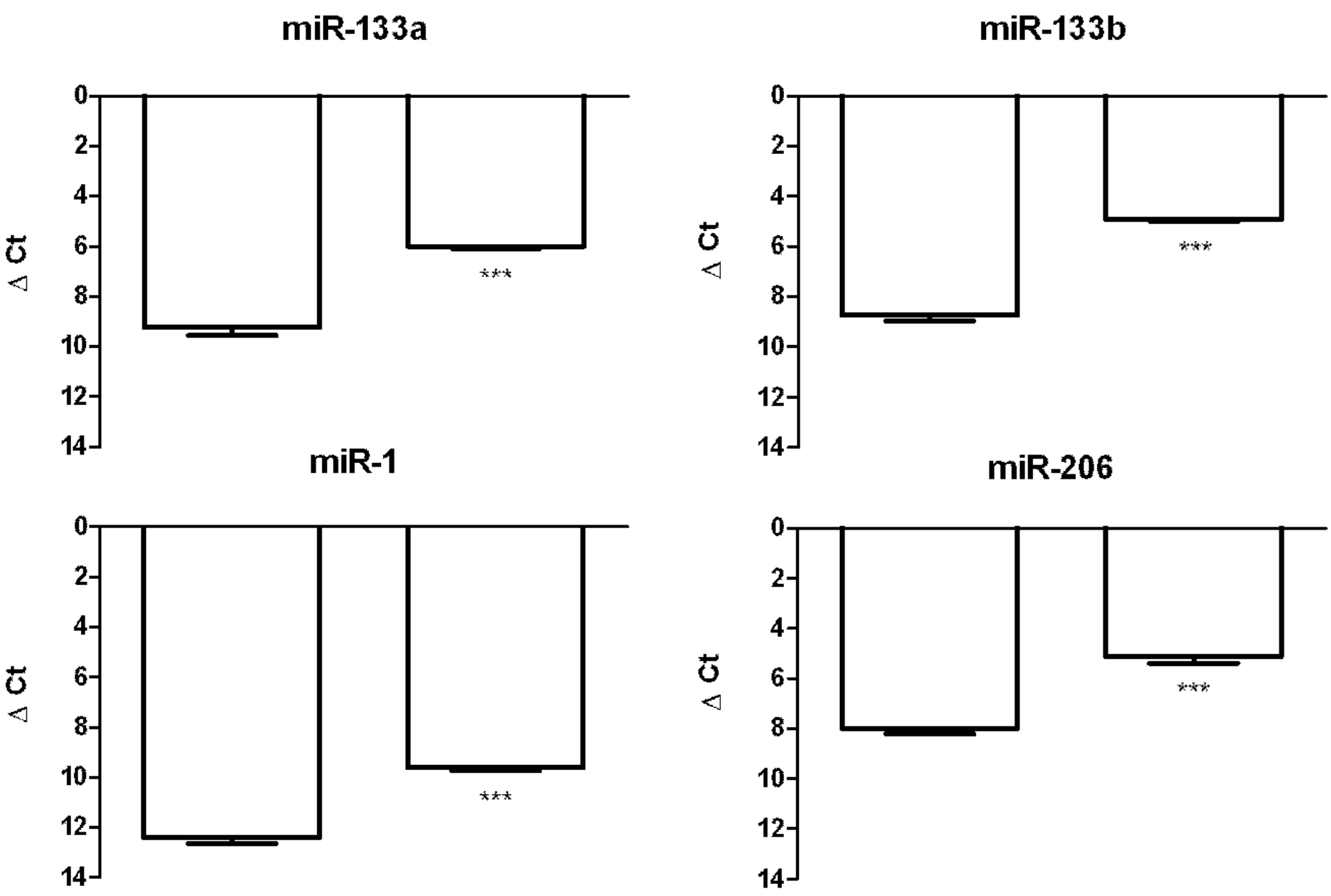
miR-133a
miR-133b
miR-1
miR-206
Δ Ct
0
2
4
6
8
10
12
14
***